WTP-49

Submitted 28 October 2008

Critical current of laminated and non-laminated BSCCO superconducting composite tape under bending strain

H. Matsubayashi[a,*], Y. Mukai[a], T. Arai[a], J. K. Shin[a], S. Ochiai[a], H. Okuda[a], K. Osamura[b], A.Otto[c], A. Malozemoff[c]

[a] Graduate School of Engineering, Kyoto University, Sakyo-ku, Kyoto 606-8501, Japan.

[b] Research Institute for Applied Sciences, Sakyo-ku, Kyoto 606 8202, Japan

[c] American Superconductor Corporation, 64 Jackson Road, Devens, MA 01434-4020, USA

Abstract

It has been reported that, when the $(Bi,Pb)_2Sr_2Ca_2Cu_3O_x$(hereafter noted as BSCCO)/Ag/Ag-alloy tape is laminated with stainless steel, the tensile strain tolerance of critical current is much improved. In this study, using the non-laminated and laminated BSCCO composite tapes fabricated at American Superconductor Corporation, the influences of lamination on the critical current and its distribution under bending strain were studied. The analysis of the measured variation of average critical current with bending strain based on the damage evolution model revealed that the laminated stainless steel acts to suppress the fracture of the BSCCO filaments.. The experimentally observed high critical current retention of the laminated tape up to high bending strain

was accounted for by the suppression of fracture of BSCCO filaments stated above and enhancement of the compressive residual strain in the filaments. The distributions of local critical current in non-laminated and laminated composite tape were described well by the three parameter Weibull distribution function within the bending strain lower than 1.1%. The coefficient of variation of distribution of critical current of the laminated tape was similar to that of the non-laminated one under the same strain distribution in the core.

PACS codes: 74.72.BK, 74.76.Bz

Keywords: BSCCO tape; Critical current; Bending; Influence of lamination

*Corresponding author:

The first author Hiroshi Mastubayashi is to be graduated in March 2009. Please contact him in the period from now to the end of February, 2009. After this period, please contact his supervisor Prof. Shojiro Ochiai whose address is also listed below.

Mr. Hiroshi Matsubayashi (Please contact with this person before the end of February, 2009)

Post address: Department of Materials Science and Engineering, Graduate School of Engineering, Kyoto University, Yoshida-Honmachi, Sakyo-ku, Kyoto 606-8501, Japan.

Phone: +81 75 753 5194,

Fax: +81 75 753 4841.

E-mail address: matubayasi.hirosi@t03.mbox.media.kyoto-u.ac.jp

Prof. Shojiro Ochiai (Please contact with this person after the end of February, 2009)

Post address: Department of Materials Science and Engineering, Graduate School of Engineering, Kyoto University, Yoshida-Honmachi, Sakyo-ku, Kyoto 606-8501, Japan.

Phone: +81 75 753 5194,

Fax: +81 75 753 4841.

E-mail address: shojiro.ochiai@materials.mbox.media.kyoto-u.ac.jp

1. Introduction

$(Bi,Pb)_2Sr_2Ca_2Cu_3O_x$(hereafter noted as BSCCO) superconducting composite tapes are subjected to mechanical and electro-magnetic stresses during fabrication and operation [1-3]. It has been reported that, when the BSCCO/Ag/Ag-alloy tape is laminated with stainless steel, the tensile strain tolerance of critical current is much improved [4-8]. The aim of the present work is to reveal the influences of lamination on the critical current under bending strain from the comparison of the experimental results between the non-laminated and laminated BSCCO composite tapes.

The present paper consists of the following contents. The experimental procedure to measure the distribution of critical current of local elements in the sample will be shown in Section 2. The experimental result of critical current distribution will be presented in Section 3.1. For analysis of the critical current - bending strain relation, the fracture strain of the BSCCO filaments will be estimated in Section 3.2, in which the enhancement of fracture strain of BSCCO filament in the laminated tape will be presented. The experimental result of the critical current - bending strain relation in both tapes will be analyzed in Section 3.3 by the damage extension model in which the estimated values in 3.3 are substituted. It will be shown that the enhancement of fracture strain of BSCCO filament in the laminated tape plays an important role for the retention of the critical current up to high bending strain. The applicability of the Weibull distribution function [9] to the distribution of the critical current in non-laminated and laminated tapes and the influence of lamination on the critical current distribution will be studied in Section 3.4.

2. Experimental procedure

In the present work, the high critical current type (noted as non-laminated sample in this work) and the high strength type (laminated sample) multifilamentary BSCCO composite tapes fabricated at American Superconductor Corporation [4] were used for test. The laminated sample was fabricated by laminating the stainless steel with the high critical current type tape as an insert tape [4]. The non-laminated sample consisting of BSCCO(Bi2223) filaments, Ag and Ag-Li alloy and the laminated sample consisting of BSCCO filaments, Ag, Ag-Li alloy and stainless steel [4] had a thickness $t_{\text{non-laminated}}$ = 0.22 mm and $t_{\text{laminated}}$ = 0.33 mm. The width of both samples was common (4.1 mm).

For measurements of a critical current distribution in these samples, 31 voltage probes were placed in a step of 10 mm with solder. Hereafter, the part of a length of 10 mm is called as an element. The samples consisting of 30 elements were wound on the cylinders with a different outer radius, R (30.1, 16.1 and 9.0 mm) through the double-faced tape with a thickness of 10 mm in order to give a bending strain, ε_{B}, at room temperature.

For the non-laminated sample, a bending strain $\varepsilon_{\text{B,non-laminated}}$ was, as in an usual manner, defined by a tensile strain at the outermost surface of a sample (Fig.1a), which is expressed by

$$\varepsilon_{B,non-la\min ated} = \frac{t_{non-la\min ated}}{2(R+1)} \quad (1)$$

On the other hand, as the bending strain for the laminated sample, we employed a tensile strain at the interface between the insert tape and stainless steel, $\varepsilon'_{\text{B,laminated}}$ (Fig.1b), instead of the tensile strain at the outermost surface of stainless steel $\varepsilon_{\text{B,laminated}}$

(Fig.1b). The $\varepsilon'_{B,laminated}$ (Fig.1b) is given by

$$\varepsilon'_{B,la\,\mathrm{min}\,ated} = \frac{t_{non-la\,\mathrm{min}\,ated}}{2(R+1)+t_{la\,\mathrm{min}\,ated}} \quad (2)$$

As the $t_{non\text{-}laminated}$ (0.22mm) was far smaller than 2(R+1) (62.2, 34.2 and 20.0 mm for R = 30.1, 16.1 and 9.0mm, respectively) in Eq.(2), Eq.(2) was practically the same as Eq.(1). ($\varepsilon_{B,non\text{-}laminated} = \varepsilon'_{B,laminated}$ = 0.35, 0.64 and 1.1%). Hereafter, both $\varepsilon_{B,non\text{-}maminated}$ and $\varepsilon'_{B,laminated}$ are noted as ε_B. Under such a definition of the bending strain ε_B, the strain distribution in an insert tape in the laminated sample was practically the same as that in the non-laminated tape (insert tape alone) for a given ε_B. Accordingly, we could directly compare a critical current of the laminated sample with that of non-laminated one under the almost same strain distribution conditions in a current transporting part.

The sample was cooled down to 77K (liquid N_2) for measurements of a voltage (V)-current (I) curve in a self-magnetic field for the 30 elements. The critical current I_c was estimated with a criterion of 1 V/m from the measured V-I curve.

3. Results and discussion

3.1. Measured distribution of critical current at ε_B = 0.35, 0.64 and 1.1%

Figs.2a and 2b shows the variations of a critical current I_c of the non-laminated and laminated samples along a sample length of 300 mm at ε_B = 0.35, 0.64 and 1.1% where ε_B refers to $\varepsilon_{B,non\text{-}laminated}$ and $\varepsilon'_{B,laminated}$ (Figs.1a and 1b). The I_c value of elements was

different to each other and an average of the critical current $I_{c,ave}$, decreased with increasing ε_B in the both samples. The reduction in $I_{c,ave}$ of the laminated sample with increasing ε_B was smaller than that of the non-laminated one.

3.2. Estimation of fracture strain of BSCCO filaments in the non-laminated and laminated samples

Tensile test for both non-laminated and laminated samples at room temperature was carried out in order to estimate the fracture strain of BSCCO filament $\varepsilon_{f,RT}$. Fig.3 shows the measured stress-strain curves. Concerning the influence of the fracture of filaments on the stress-strain curve, the following features have been revealed [10,11]. (1) The stress carrying capacity of a composite is reduced when filaments are fractured. Accordingly, the slope of the stress-strain curve is reduced in comparison with the extrapolation of the slope in a region where no filaments are fractured. (2) A stress is transferred even to the once-fractured filaments. As a result, once-fractured filaments are fractured again. Such a process is repeated continually, resulting in multiple fracture of filaments. In such a stage, the stress-strain curve becomes almost flat. (3) Accordingly, the strain, at which the filaments are fractured for the first time, can be identified as a strain at deviation of the slope in the region which appears in advance of a flat portion in a stress-strain curve. (4) The strain at fracture of filaments in the composite tape is expressed by $\varepsilon_{f,RT}$- $\varepsilon_{r,RT}$ where the $\varepsilon_{f,RT}$ and $\varepsilon_{r,RT}$ are an intrinsic fracture strain and a residual strain of BSCCO filament at room temperature, respectively. Applying these features to the measured stress-strain curves in Fig.3, the strains surrounded by the circles correspond to $\varepsilon_{f,RT}$- $\varepsilon_{r,RT}$, which are read to be 0.12 and

0.33% for the non-laminated and laminated samples, respectively. The values of $\varepsilon_{r,RT}$ of the non-laminated and laminated samples have been estimated to be -0.05 and -0.13%, respectively, by an X-ray diffraction experiment in our former work [12]. From these values, the values of $\varepsilon_{f,RT}$ of the non-laminated and laminated samples were estimated to be 0.07 and 0.20%, respectively. Not only the $\varepsilon_{r,RT}$ value but also the $\varepsilon_{f,RT}$ one was quite different between the non-laminated and laminated samples. In this way, the lamination acts not only to enhance a compressive residual strain but also to suppress a fracture of filaments.

3.3 Description of an average critical current-bending strain relation with the values of $\varepsilon_{f,RT}$ and $\varepsilon_{r,RT}$ estimated in 3.2.

The normalized critical current I_c/I_{c0} for $\varepsilon_B > \varepsilon_{B,irr}$ (irreversible bending strain) is approximately given by

$$\frac{I_c}{I_{c0}} = \frac{1}{2}\left(1 + \frac{\varepsilon_{f,RT} - \varepsilon_{r,RT}}{\varepsilon_B V_{sc}}\right) \quad (3)$$

[13-15] where I_{c0} is the original critical current at $\varepsilon_B = 0$ (=160 and 135A in the non-laminated and laminated samples, respectively) and V_{sc} is the volume fraction of the core where the filaments that transport current are embedded in Ag (=0.67 in the both samples in the present approach using $\varepsilon_B = \varepsilon_{B,non\text{-}laminated}$ for non-laminated sample and $= \varepsilon'_{B,laminated}$ for laminated sample (Fig.1)). In this section, we analyze a relation of the average I_c/I_{c0} value to bending strain ε_B by substituting $\varepsilon_{f,RT}$ - $\varepsilon_{r,RT}$ = 0.12%

(non-laminated sample) and 0.33%(laminated sample) estimated in 3.2. The value of I_c/I_{c0} of the laminated sample at ε_B = 0.35% is 1.0 because of $\varepsilon_{B,irr} > 0.35\%$. Figs.4a and 4b show a comparison of the calculated I_c/I_{c0} with the measured one. The calculated I_c/I_{c0} values for both samples describe fairly well the measured ones at all bending strains investigated. Fig.4b also shows the values of I_c/I_{c0} of the laminated sample calculated with $\varepsilon_{f,RT}$ = 0.07% (the value of non-laminated sample) for reference. The calculated I_c/I_{c0} values were too low to describe the measured values at ε_B = 0.64 and 1.1%, indicating again the $\varepsilon_{f,RT}$ value was improved by the lamination. From these results, it is concluded that an improvement of the fracture stain of BSCCO filaments by the lamination contributed largely to a retention of high critical current at high bending strain in the laminated sample.

3.4 Distribution of critical current in the non-laminated and laminated samples

It has been shown that the Weibull distribution is a useful tool for description of a critical current distribution [10, 13-15]. In this section, first, whether the critical current distribution of the non-laminated and laminated samples is described by this function or not was examined, and, based on the result, influences of lamination on the distribution of the critical current were studied.

According to the three-parameter Weibull distribution function, a cumulative probability F of critical current I_c with a length 10mm is expressed by

$$F = 1 - \exp\left[-\left\{ \frac{\left(I_c - I_{c,\min}\right)}{I_0} \right\}^m \right] \quad (4)$$

where $I_{c,min}$ is the minimum (lower limit) I_c value below which there is no I_c value (F=0), I_0 the scale parameter and m the shape parameter. Equation (4) is rewritten as

$$\ln\ln\left\{(1-F)^{-1}\right\} = m\ln\left(I_c - I_{c,\min}\right) - m\ln\left(I_0\right) \quad (5)$$

From a regression analysis of the plot of $\ln\ln\{(1-F)^{-1}\}$ against $\ln(I_c-I_{c,min})$, the values of m, $I_{c,min}$ and I_0 were estimated for non-laminated and laminated samples, as shown in Table.1 and Table.2. The cumulative probability F and then the probability density f were calculated as a function I_c by substituting the estimated values mentioned above into Eq.(4). The calculated f-I_c curves are presented in Fig.5a,b. The experimental results of both samples were well described by the three parameter distribution function with the estimated parameter values.

The coefficients of variation (COV) of the critical current of the non-laminated sample were 0.015, 0.016 and 0.024 and those of the laminated sample were 0.011, 0.022 and 0.017 at ε_B = 0.34, 0.65 and 1.1%, respectively. The COV values at all bending strains were almost on the same level. This result means that the influence of lamination on the COV was minor under bending strain, while it was large under tensile strain [8].

4. Conclusions

(1) The critical current values of the bent laminated sample were far higher than those of the bent non-laminated sample for the same strain distribution in the core.

(2) The analysis of the stress-strain curve and variation of average critical current with

bending strain for both laminated and non-laminated samples revealed that the fracture of BSCCO filaments was suppressed by the laminated stainless steel.

(3)The experimental results mentioned in (1) were accounted for by the suppression of fracture of Bi2223 filaments mentioned in (2) and by the enhancement of compressive residual strain in BSCCO filaments in the laminated sample.

(4) The distributions of critical current both of non-laminated and laminated samples were described well by a three parameter Weibull distribution function with different parameter values. The coefficient of variation of distribution of critical current of the laminated sample was similar to that of the non-laminated one.

Acknowledgements

The authors wish to express their gratitude to The Ministry of Education, Culture, Sports, Science and Technology, Japan and to NEDO (New Energy and Industrial Technology Development Organization, Japan) for the grant-in-aid.

References

[1]P. Vase, R. Flükiger, M. Leghissa, B. Glowacki, Supercond. Sci. Technol. 13(2000) R71.

[2] H. Kitaguchi, K. Itoh, H. Kumakura, T. Takeuchi, K. Togano, W. Wada, IEEE Trans. Appl. Supercond. 11(2001)3058.

[3] H. J. N. van Eck, K. Vargast, B. ten Haken, and H. H. J. ten Kate, Supercond. Sci. Technol. 15(2003)1213.

[4] A. Otto, E.J. Harley, R. Mason, Supercond. Sci. Technol. 18 (2005) S308

[5] L. J. Masur, D. Buczek, E. Harley, T. Kodenkandath, X. Li, J. Lynch, N. Nguyen, M.

Rupich, U. Schoop, J. Scudiere, E. Siegal, C. Thieme, D. Verebelyi, W. Zhang, J. Kellers, Physica C 392-396 (2003)989.

[6] M. Buczek, L. J. Masur, P. K. Miles, F. Sivo, D. Marlowe, E. R. Podtburg, D. I. Parker, J. D. Scudiere, P. Metra, M. Nassi, M. Rahman, D. W. Von Dollen, IEEE Trans. Appl. Supercond. 7 (1997)2196.

[7] A. Salazar, J. K. Pastor, J. Llorca, IEEE Trans. Appl. Supercond. 14 (2004)1941-47.

[8] Y. Mukai, J.K. Shin, S. Ochiai, H. Okuda, M. Sugano, K. Osamura, Physica C 468 (2008) 1801

[9] W. J. Weibull, Appl. Mech. 28 (1951) 293

[10] S. Ochiai, J. K. Shin, S. Iwamoto, H. Okuda, S. S. Oh, D. W. Ha, M. Sato, J. Appl. Phys. 103(2008) 123911.

[11] S. Ochiai, T. Matsuoka, J. K. Shin, H. Okuda, M. Sugano, M. Hojo, K. Osamura, Supercond. Sci. Technol. 20(2007)1076.

[12] S. Ochiai, H. Rokkaku, J.K. Shin, S. Iwamoto, H. Okuda, K. Osamura, M. Sato, A. Otto, A. Malozemoff, Supercond. Sci. Technol. 21 (2008) 075009

[13] S. Ochiai, M. Fujimoto, J.K. Shin, H. Okuda, M. Hojo, K. Osamura, T. Kuroda, K. Itoh, H. Wada, Physica C 463-465 (2007) 885

[14] S. Ochiai, J.K. Shin, Y. Mukai, H. Matsubayashi, H. Okuda, M. Sugano, M. Hojo, K. Osamura, T. Kuroda, K. Itoh, H. Wada, Physica C 468 (2008) 1796

[15]S. Ochiai, J. K. Shin, H. Okuda, M. Sugano, M. Hojo, K. Osamura, T. Kuroda, K. Itoh, H. Wada, Supercond. Sci. Technol. 21(2008) 054002

Table.1 Estimated values of m, $I_{c,min}$ and I_0 in the non-laminated sample.

	m	$I_{c,min}$(A)	I_0(A)
ε_B=0.35%	7.5	111	13
ε_B=0.64%	8.4	88	12
ε_B=1.1%	6.8	73	13

Table.2 Estimated values of m, $I_{c,min}$ and I_0 in the laminated sample.

	m	$I_{c,min}$(A)	I_0(A)
ε_B=0.35%	4.9	128	7.0
ε_B=0.64%	5.1	113	14
ε_B=1.1%	5.6	99	10

Figure Captions

Fig.1 Schematic representation of the transverse cross-section and the definition of the bending strain. (a) Non-laminated sample. (b) Laminated sample.

Fig.2 Measured variations of critical current at ε_B = 0.35, 0.64 and 1.1%. (a) Non-laminated sample. (b) Laminated sample.

Fig.3 Measured stress-strain curves of the non-laminated and laminated sample at room temperature. The broken lines show the slope of the region in which the BSCCO filaments were not fractured. The circles show the strain at which the fracture of BSCCO filaments took place.

Fig.4 Comparison of the calculated normalized critical current I_c/I_{c0} at ε_B = 0.35, 0.64 and 1.1% with the measured ones. (a) Non-laminated sample. (b) Laminated sample.

Fig.5 Measured (histogram) and analyzed (solid curve) distributions of critical current. (a) Non-laminated sample. (b) Laminated sample.

Fig

.1

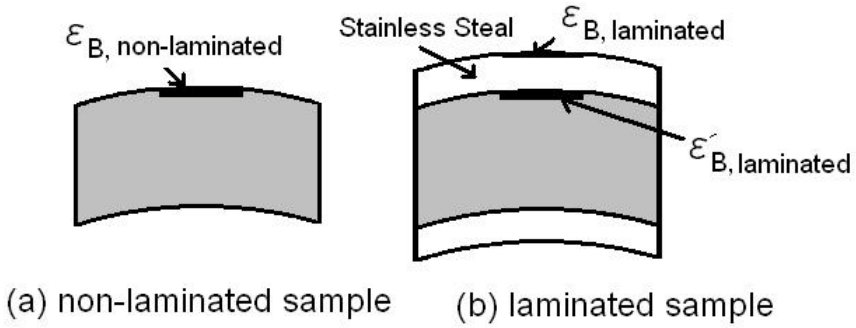
$\varepsilon_{B,\ non\text{-}laminated}$
Stainless Steal
$\varepsilon_{B,\ laminated}$
$\varepsilon'_{B,\ laminated}$
(a) non-laminated sample
(b) laminated sample

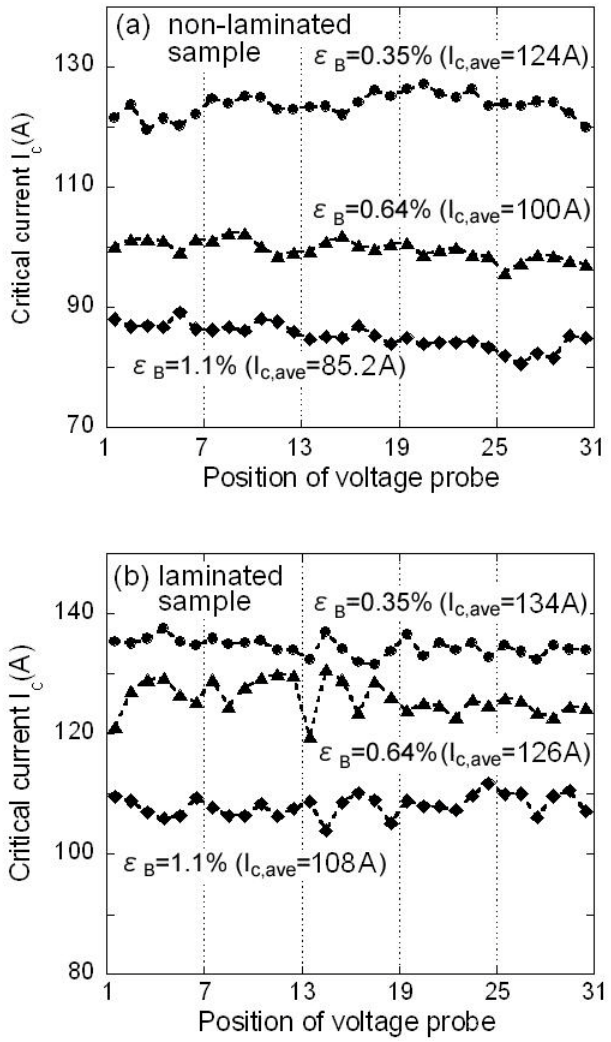
(a) non-laminated sample
ε_B=0.35% ($I_{c,ave}$=124A)
ε_B=0.64% ($I_{c,ave}$=100A)
ε_B=1.1% ($I_{c,ave}$=85.2A)
Critical current I_c (A)
Position of voltage probe
(b) laminated sample
ε_B=0.35% ($I_{c,ave}$=134A)
ε_B=0.64% ($I_{c,ave}$=126A)
ε_B=1.1% ($I_{c,ave}$=108A)
Critical current I_c (A)
Position of voltage probe

Fig.2

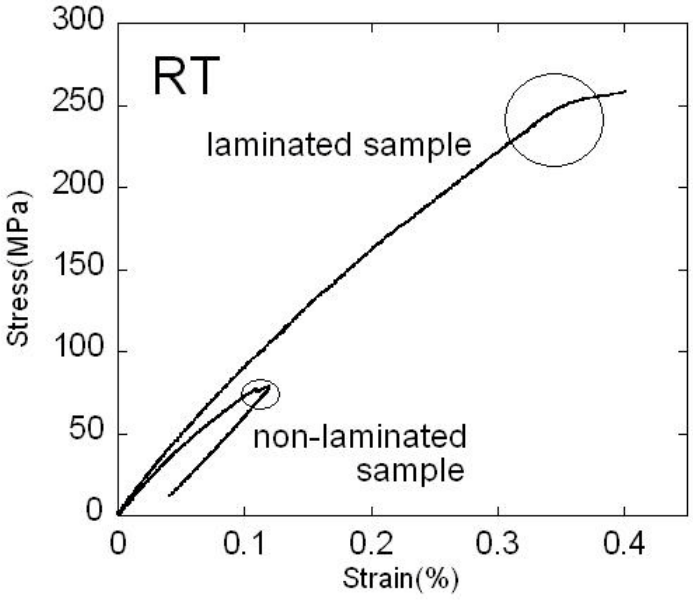
RT
laminated sample
non-laminated
sample
Stress(MPa)
Strain(%)
300
250
200
150
100
50
0
0
0.1
0.2
0.3
0.4

Fig.3

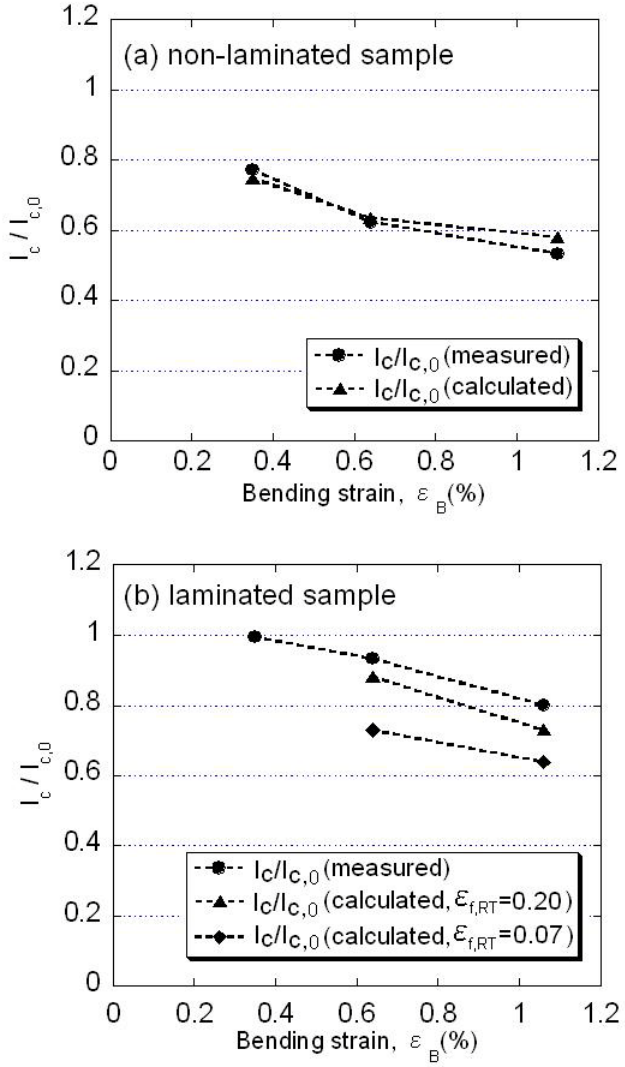
(a) non-laminated sample
$I_c / I_{c,0}$
Bending strain, ε_B(%)
$I_c/I_{c,0}$(measured)
$I_c/I_{c,0}$(calculated)
(b) laminated sample
$I_c / I_{c,0}$
Bending strain, ε_B(%)
$I_c/I_{c,0}$(measured)
$I_c/I_{c,0}$(calculated, $\varepsilon_{f,RT}$=0.20)
$I_c/I_{c,0}$(calculated, $\varepsilon_{f,RT}$=0.07)

Fig.4

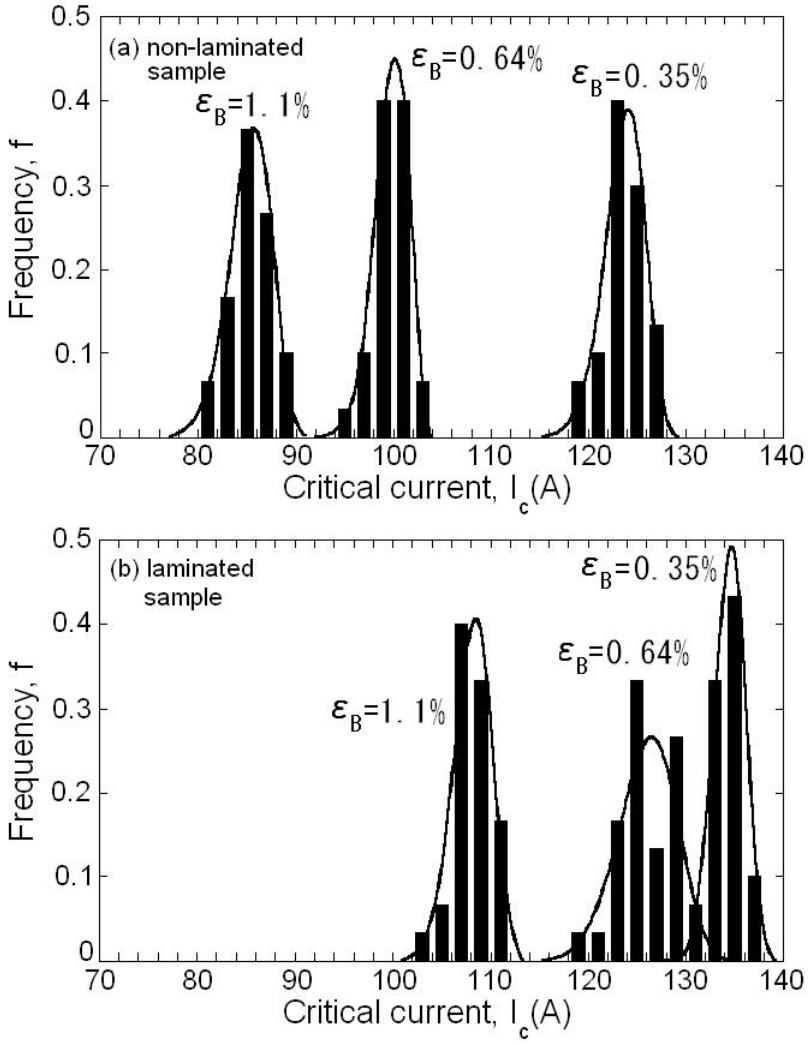
(a) non-laminated sample
ε_B=1. 1%
ε_B=0. 64%
ε_B=0. 35%
Frequency, f
Critical current, I_c(A)
(b) laminated sample
ε_B=0. 35%
ε_B=0. 64%
ε_B=1. 1%
Frequency, f
Critical current, I_c(A)

Fig.5